Optimizing regenerative braking

by I Nyoman Sutantra

Submission date: 19-May-2022 07:25PM (UTC+0700)
Submission ID: 1839790735
File name: budijono_ijpeds_2.docx (550.57K)
Word count: 4071
Character count: 22184

Optimizing regenerative braking on electric vehicles using a model-based algorithm in the antilock braking system

I Nyoman Sutantra[1], Agus Sigit Pramono[1], Agung Prijo Budijono[2,3]
[1]Department of Mechanical Engineering, Faculty of Industrial Technology, Institut Teknologi Sepuluh Nopember, Surabaya, Indonesia
[2]Department of Mechanical Engineering, Faculty of Engineering, Universitas Negeri Surabaya, Surabaya, Indonesia
[3] Mechanical Design System Research Group, Institut Teknologi Sepuluh Nopember, Surabaya, Indonesia

Article Info

Article history:

Received mm dd, yyyy
Revised mm dd, yyyy
Accepted mm dd, yyyy

Keywords:

Regenerative braking
Electric vehicles
Antilock braking system
Model-based algorithms
Friction frequency
Harvesting energy

ABSTRACT

The regenerative braking efficiency of electric vehicles (EVs), with 8 - 25% range, challenges designers to create better braking systems. The antilock braking system (ABS) was chosen because it has many advantages, such as superior safety factors, the ability of the vehicle to maneuver, and so on. The measurement results showed that ABS took longer to make the wheels stop with the same wheel rotation speed. It caused lower induced emf in the generator due to its lower differentiation of magnetic flux to time. ABS 50 Hz performance showed 19.5% at 4500 pm, while hydraulic brake performance was 21% at the same speed. Model-based algorithms (MBAs) were used in ABS to increase the friction frequency with the wheels from 10 to 50 Hz. This increase in frequency caused the ABS graph to approach the hydraulic graph, that the ABS performance increased. Although ABS loses to hydraulics in stopping wheel rotation, it wins in stored energy and temperature in the battery. Longer wheel stop times give the wheel rotational kinetic energy more time to convert into electricity.

1. INTRODUCTION

Electric vehicles (EVs) are a solution to reduce air pollution and fuel consumption caused by combustion motors [1]. Also, EVs have higher efficiency than combustion motors due to recovering energy during operation. One way to restore is to use regenerative braking [2]. Regenerative braking utilizes kinetic energy in the braking process where the wheels are still rotating even though braking has been applied. This kinetic energy is converted into electrical energy and stored in batteries. Therefore, regenerative braking is limited by vehicle speed and the battery state of charge (SOC) [3]. Also, vehicle stability and energy recovery as much as possible are factors for allocating braking torque [4].

It is undeniable that vehicle accidents on the highway caused by braking have claimed many lives. Two things that could be adjusted on the vehicle's dynamic control were the antilock brake system (ABS) and the traction control system (TCS) [5]. ABS provides a solution for vehicle stability. The driver can still control the vehicle during the braking process. The constancy of ABS is because it has an algorithm for controlling hydraulic pressure in the brakes, which can be divided into two categories, Model-Based Algorithms (MBAs) and Rule-Based Algorithms (RBAs) [6]. The MBA mathematically models the braking process and requires a lot of data input. It is more accurate. Meanwhile, RBA bases its algorithm on the relevant variables on the control action. It is simpler.

In this study, based on the application of regenerative braking in EVs, we used powertrain components (induction motor, generator, and battery) to simulate it. Accuracy in the placement of powertrain components will increase the vehicle's NVH (Noise, Vibration, and Harshness) behaviour [7]. The induction motor rotated the driving wheel (DW) through the pulley in a ratio of one to obtain the same torque. The energy captured (ECW) shaft got double the speed of the DW axle because the gears had a comparison of two, as shown in Figure 1. The different axles allowed for more stable rotation [8], and double speed meant more fluxes for the generator [9].

The remainder of the paper contains section 2 explaining how regenerative braking works on the Antilock Braking System (ABS). Section 3 describes the components of the regenerative braking process of this study. The results of measurements and speed calculations are presented in section 4. Last, section 5 gives the best regenerative braking conclusion.

2. RELATED WORK

EVs are closely related to regenerative braking because the energy lost due to the braking process ranges from 30% to 50% [10]. Regenerative braking can provide recovery of 8% to 25% [11]. This range challenges designers to create high-efficiency regenerative braking. Frictional braking system (FBS) and regenerative braking system (RBS) are the two braking systems on current EVs. FBS is a conventional system. RBS brakes the motor and converts the kinetic energy into electricity to charge the battery. In addition, structural reconstruction is required in regenerative braking to separate pedal force and brake pressure [12]. It is usually called a brake-by-wire system, and braking effectiveness increases.

Accurate braking required real-time identification of road conditions [13]. It would be used as a reference in determining the braking torque. The ABS controlled this torque to achieve wheel-slip based on the wheel-deceleration approach. Also, ABS used a motor to drive the actuator arm [14]. It provided controllable torque all the time. This control used the Kalman filter algorithm in real-time, where the wheel speed estimation was processed based on the signals obtained by the wheel-speed sensor [15]. This algorithm was also produced to increase the precision in speed estimation on composite braking systems.

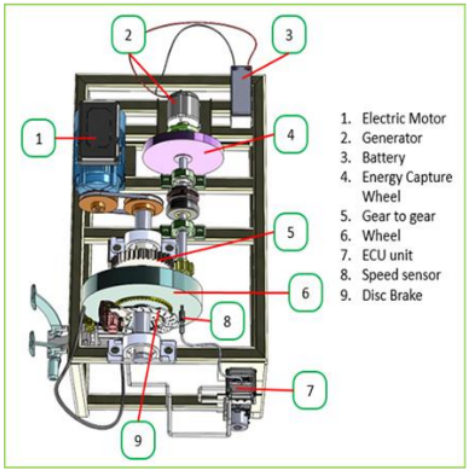

Figure 1. Experimental configuration

3. METHOD

3.1 Powertrain components

Current technological developments force people to produce motors with specifications of high speed, high capacity, high accuracy, and high efficiency. One effort to fulfil this is to combine two or more eccentric motors [16]. The result satisfies the above conditions, but it causes vibration problems. The use of multiple shafts can solve this problem. The addition of a pulley to connect the two axles minimizes the resulting vibration. Table 1 shows the specifications of the DC induction motor used in this study.

Table 1. Motor DC specifications

Voltage	48 V
Power	350 W
Current	9.4 A
Load (max)	350 kg
Torque	1.5–7.5 N.m
Speed	500 – 2750 rpm
Ratio	1:5

The relationship between power, torque and speed of the motor is as follows:

$$P = \frac{2\pi nT}{60} \quad (1)$$

Where P is power in Watt, n is the speed in rpm, and T is torque in N.m.

A motor-driven generator is a converter of kinetic energy into electrical energy. It requires a high magnetic flux to produce a stable electric current. It could not be provided by regenerative braking because the rotation of the shaft in the braking process decreased. High flux concentrations can be created by chamfering the ends of the stator feet [17]. Another way is to increase the rotational speed of the drive shaft by giving the gear ratio. The DC generator specifications are listed in Table 2.

Table 2. Generator DC specifications

Voltage	24 V
Power	250 W
Current	16.4 A
Load (max)	350 kg
Speed rate	2700 rpm

The induced emf and the electric current generated by the generator are presented by Equations (2) and (3), respectively.

$$\varepsilon_{ind} = -N\frac{d\phi}{dt} \quad (2)$$

$$I_{ind} = \frac{\varepsilon_{ind}}{R} \quad (3)$$

Where ε_{ind} is the induced emf in Volts, N is the number of windings, ϕ is the magnetic flux, t is the time, I_{ind} is the induced current in Ampere, and R is the resistance in Ω.

Battery storage capacity is the next obstacle that can reduce efficiency. The problem that is often experienced was the occurrence of electrical overloading (EOL) during the filling process on the track. One of the causes was excess torque on the rotating shaft of the generator, and no recovery phase was available [18]. Therefore, there is a need for interaction between charge control, on-track power management, and mitigating battery power degradation [19]. It can increase efficiency as desired.

3.2 Antilock braking system (ABS)

ABS is an active safety system for vehicles [20]. The firm factors that affect its safety were the tire design parameters and operating conditions on the tire force characteristics [21]. It can maintain the slip ratio at some value to avoid locking the tires, thereby maximizing friction potential [22]. Friction in the braking process can be used to charge the battery instead of being discharged as heat [23]. Vehicle energy is lost about 20 to 70% during braking [24]. Modeling and simulation are carried out to create performance and safety in automotive [25].

Slip ratio is a determining parameter in ABS using MBA. Figure 2 below is the result of previous research, which shows the relationship between braking force and slip ratio based on road conditions. Road conditions were a complex factor to predict. It was only approachable.

The sliding surface caused by the friction forces during the braking process can be written as

$$s = F_x(\kappa) + \beta(t) \quad (4)$$

where s is the sliding surface variable in m, F_x is the frictional force in N, κ is the slip ratio, and $\beta(t)$ is the function of increasing time in the self-optimization algorithm. $\beta(t)$ can be written as

$$\beta(t) = \rho.t \quad (5)$$

where ρ is a positive constant in the self-optimization algorithm, and t is the time variable. When the wheel stops, $\dot{s} = 0$. The result of this condition can be written as $F_x = -\rho$, which means that the frictional force will always increase.

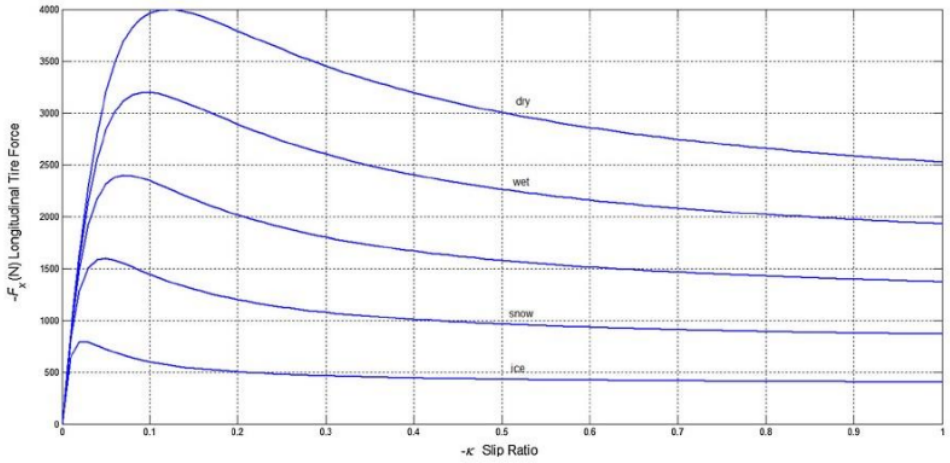

Figure 2. The relationship between tire friction and slip ratio for some road conditions (It taken from [22])

The derivative of Equation (4) is

$$\dot{s} = \frac{dF_x(\kappa)}{d\kappa}\dot{\kappa} + \rho \tag{6}$$

The gradient $\frac{dF_x(\kappa)}{d\kappa}$ depends on the road conditions because the road conditions are unknown. Selection of $\dot{\kappa}$ function to ensure $\dot{s} = 0$ is

$$\dot{\kappa} = M\ \mathrm{sgn}\left[\sin\left(\frac{\pi s}{\gamma}\right)\right] \tag{7}$$

If the following form

$$\left|\frac{dF_x(\kappa)}{d\kappa}\right| > \frac{\rho}{M} \tag{8}$$

is true so M and γ in Equations (7) and (8) are positive constants in the self-optimization algorithm.

The gradient $\frac{dF_x(\kappa)}{d\kappa}$ in Equation (6) is unknown, so the sign for the function $\dot{\kappa}$ is also the same. The literature refers to it as a control with the direction of the control vector uncertain. By plugging Equation (7) into Equation (6) as

$$\dot{s} = \frac{dF_x(\kappa)}{d\kappa} M\ \mathrm{sgn}\left[\sin\left(\frac{\pi s}{\gamma}\right)\right] + \rho \tag{9}$$

satisfy the variable of sliding at the start of the optimization as

$$\gamma < s(0) < 2\gamma \tag{10}$$

The assumption is intended to show the truth of the spacing then it will be correct for all ranges of s. The spacing in Equation (10) can be expressed mathematically as

$$\mathrm{sgn}\left[\sin\left(\frac{\pi s}{\gamma}\right)\right] = -\mathrm{sgn}(s - \gamma) \tag{11}$$

and,

$$\mathrm{sgn}\left[\sin\left(\frac{\pi s}{\gamma}\right)\right] = \mathrm{sgn}(s - 2\gamma) \tag{12}$$

then combine Equations (9) and (11)

$$\dot{s} = -\frac{dF_x(\kappa)}{d\kappa} M \operatorname{sgn}(s-\gamma) + \rho \tag{13}$$

Defines a variable λ as

$$\lambda = s - \gamma \tag{14}$$

and since γ is constant, then

$$\dot{\lambda} = \dot{s} \tag{15}$$

Equation (13) becomes

$$\dot{\lambda} = -\frac{dF_x(\kappa)}{d\kappa} M \operatorname{sgn}(\lambda) + \rho \tag{16}$$

Multiplying both sides of Equation (16) by λ becomes inequality

$$\lambda\dot{\lambda} \le -|\lambda| \left[\frac{dF_x(\kappa)}{d\kappa} M - \rho\right] \tag{17}$$

If condition $\frac{dF_x(\kappa)}{d\kappa} M > \rho$ is correct, the right-hand part of Equation (17) becomes negative. It means that λ will be zero at a finite time. The following values will be true

$$\lambda = 0, \quad s = \gamma \tag{18}$$

Another alternative solution is to combine Equations (9) and (12)

$$\dot{s} = \frac{dF_x(\kappa)}{d\kappa} M \operatorname{sgn}(s-2\gamma) + \rho \tag{19}$$

Definition of λ as

$$\lambda = s - 2\gamma \tag{20}$$

Equation (19) is defined as

$$\dot{s} = \frac{dF_x(\kappa)}{d\kappa} M \operatorname{sgn}(\lambda) + \rho \tag{21}$$

With the same treatment, the following inequalities occur:

$$\lambda\dot{\lambda} \le |\lambda| \left[\frac{dF_x(\kappa)}{d\kappa} M + \rho\right] \tag{22}$$

When the conditions $\frac{dF_x(\kappa)}{d\kappa} M = -\rho$ in Equation (22) are correct, λ approaches zero in a finite time, and the following forms are met:

$$\lambda = 0, \quad s = 2\gamma \tag{23}$$

The above analysis applies not only to Equation (10) but also to all ranges. Whatever the value of s will be as follows

$$s = k\gamma; \quad (k = 0, \pm 1, \pm 2, \dots) \tag{24}$$

The value of k is constant. It means

$$s = k\gamma = F_x(\kappa) + \rho t \tag{25}$$

$$F_x(\kappa) = -\rho t + k\gamma \tag{26}$$

The derivative to time in Equation (26) produces

$$\dot{F}_x(\kappa) = -\rho \tag{27}$$

The graph Equation (9) with the conditions Equation (8) is presented in Figure 3. Figure 3a for condition $dF_x(\kappa)/d\kappa > \rho/M$ and Figure 3b for condition $dF_x(\kappa)/d\kappa < -\rho/M$ as follows.

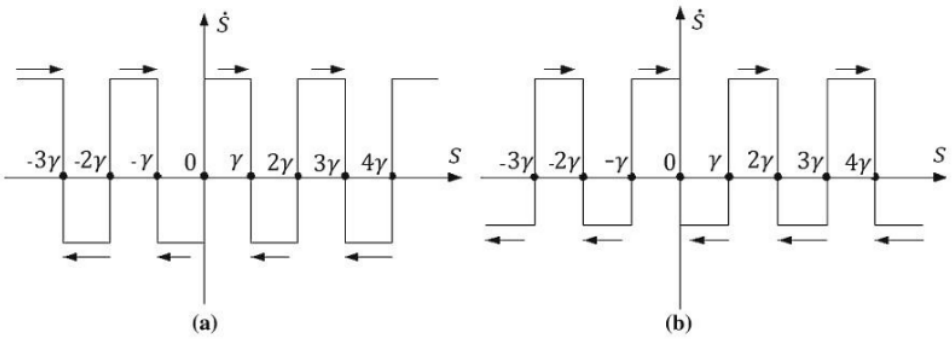

Figure 3. Changes in s and $\dot{s}$ based on Equation (9) (a) for $dF_x(\kappa)/d\kappa > \rho/M$, (b) for $dF_x(\kappa)/d\kappa < -\rho/M$

3.3 Hydraulic braking

EVs also adopted a blended braking system. It contained a hydraulic system as the driving force to obtain a more optimal braking process. The control for the system also used the extended Kalman filter algorithm to make the powertrain more flexible [26]. Regenerative braking plus a hydraulic is usually used on trucks with hydraulic carriers [27]. The regenerative breaking results stored in the battery were used to drive the hydraulic arm.

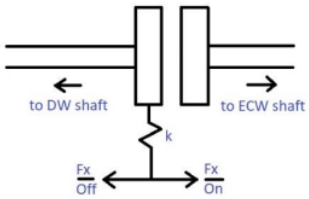

Figure 4. Centrifugal structure in clutch used

3.4 Clutch

EVs still use a dual-clutch transmission (DCT) though usually only on conventional vehicles because it has high efficiency and a compact structure [28]. It can also eliminate the need for a torque converter if it uses two clutches simultaneously. Also, it can significantly improve ride comfort, utilize full motor power, reduce engine ing, and optimize engine operating points [29]. In addition, a combined DCT was also developed with a control algorithm for efficient shifting and launching [30]. Figure 4 illustrates the clutch used. The centrifugal structure ensured that only the braking torque was connected to the ECW.

4. RESULTS AND DISCUSSION

The study used an induction motor that was gradually loaded. It produced a shaft rotation starting at 500 rpm and increasing by 250 rpm until it reached a maximum rotation of about 2250 rpm. Disc brakes were applied to the DW using conventional hydraulic brakes and ABS. Pressure on the brake piston was set at 2 kg/mm2. ABS was controlled using a module included in the electronic control unit (ECU). This control was

modified using an MBA, in which the frequency on the ABS increased from 10 Hz to 50 Hz. This increase resulted in the replacement of the microcontroller for each frequency. The results are presented in Figure 5.

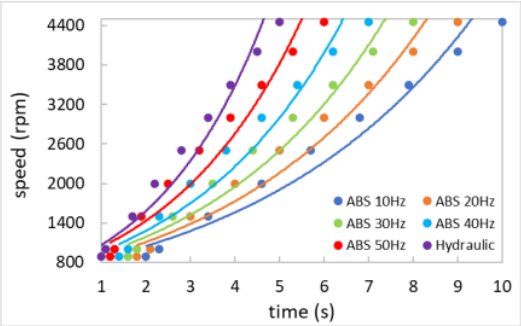

Figure 5. Speed measurement

The speed ratio between ECW and DW was 2. It was applied to make the generator rotate faster and produces a higher electric current. ABS provided a longer wheel stop time than hydraulics. The safety factor in ABS, which avoids wheel locking, caused this time extension. However, the driver can still control the vehicle with actuators [31]. There is a relationship between braking force and wheel slip ratio in ABS [32], as shown in Figure 2.

Hydraulic braking had the shortest time to stop the wheels. It is due to the mechanism that immediately grips the wheel and does not release it at all. This mechanism creates the highest friction, and the wheel converts its kinetic energy into heat quickly. This sudden change will affect the induced current of the generator and the torque of the shaft that rotates it. Furthermore, hydraulics is used in heavy vehicles because of their strength [33].

Increasing the frequency of ABS shortens braking time. The periodic graph interval causes the friction intensity to escalate and makes the ABS graph close to the hydraulic graph. An increase in ABS frequency brings ABS closer to hydraulics of stopping the wheel. However, ABS provides more safety and maneuverability at high speeds [34]. The power calculation on the generator is presented in Figure 6.

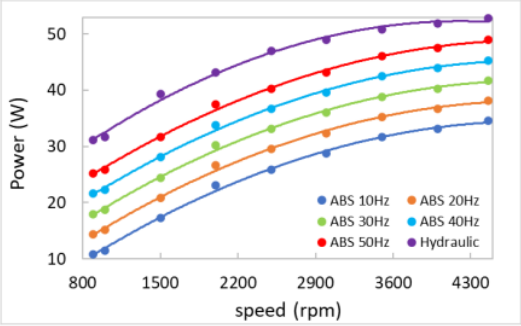

Figure 6. Power on generator calculation

The highest magnetic flux through the generator was achieved by hydraulics. The change in hydraulic induced emf based on Equation (2) was the fastest because it has the shortest braking time. It caused the highest induced current to flow into the battery. The highest power produced the tallest torque, according to Equation (1), and the highest performance. Torque calculation is shown in Figure 7.

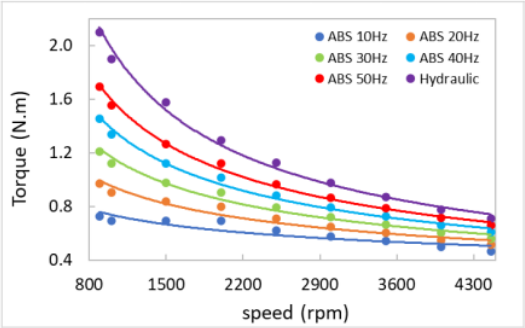

Figure 7. Torque on ECW calculation

Torque depends on ECW shaft power. The generator connected to the ECW is up to 250 W of power, as shown in Table 2. The highest generator power in hydraulic braking ranges from 30 to 50 W, as presented in Figure 6, indicating that the efficiency is 12 to 21%. Graphs in Figure 7 are the shaft torque that rotates the generator and are the torque available in the regenerative braking process.

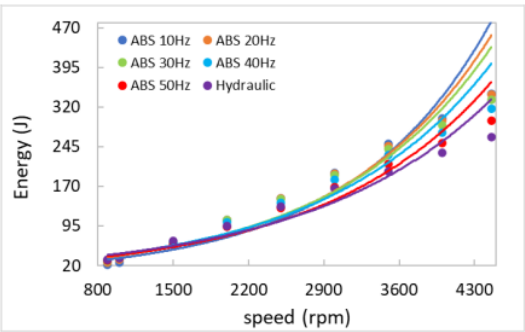

Figure 8. Energy on battery calculation

Different phenomena occur in energy graphs, as indicated in Figure 8. 10 Hz ABS has the highest energy in harvesting energy during regenerative braking. It has the longest time stopping the wheel and produces the most electricity accumulated in the battery. The longest time indicates that the kinetic energy of the wheel rotation turns into electrical instead of being lost to heat due to friction.

The 10 Hz ABS has the lowest energy stored in the battery at low revolutions, as Figure 8 shows. It is due to the insignificant time difference in the braking power. Harvesting energy at low speed is dominated by generator power, while wheel stop time takes over at high-speed.

No less important than the battery is the cooling system [18]. There is a relationship between electric current and battery temperature. The higher the electricity, the higher the battery temperature [19]. Figure 9 shows the results of measuring battery temperature during harvesting energy from regenerative braking. The hydraulics give the battery the highest temperature because it has the highest current.

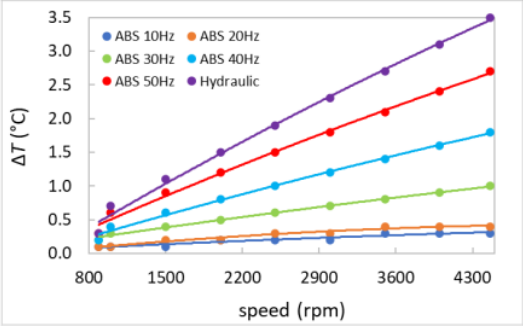

Figure 9. Measurement of battery temperature

5. CONCLUSION

EVs offer a solution for saving fossil fuels and preventing environmental damage. In addition, conventional vehicles have lower efficiency in power usage than EVs. EVs can recover energy in several ways, one of which is regenerative braking. The braking system used for regenerative braking is similar to conventional vehicles, with hydraulic brakes and ABS. ABS has a module that contains an algorithm to control the friction between brake and wheel and makes it safer than hydraulic brakes.

The long wheel-stopping time of ABS prevents the wheels from slipping during the braking process. It results in the highest harvesting energy in ABS because it allows a lot of the kinetic energy of wheel rotation to be converted into electricity. However, the generator power in ABS is low because of the low induced current. Lowly potency is advantageous because it does not cause the battery to heat up quickly.

REFERENCES

[1] Y. Zhang, W. Wang, C. Xiang, C. Yang, H. Peng, and C. Wei, "A swarm intelligence-based predicitve regenerative braking control strategy for hybrid electric vehicle," *Vehicle System Dynamics*, doi: 10.1080/00423114.2020.1845387.

[2] N. Bosso, M. Magelli, and N. Zampieri, "Application of low-power energy harvesting solutions in the railway field: a review," *Vehicle System Dynamics*, vol. 59, no. 6, pp. 841–871, 2021, doi: 10.1080/00423114.2020.1726973.

[3] K. V. Subramaniyam and S. C. Subramanian, "Impact of regenerative braking torque blend-out characterictics on electrified heavy road vehicle braking performance," *Vehicle System Dynamics*, vol. 59, no. 2, pp. 269–294, 2021, doi: 10.1080/00423114.2019.1677921.

[4] F. Sun, W. Liu, H. He, and H. Guo, "An integrated control strategy for the composite braking system of an electric vehicle with independently driven axles," *Vehicle System Dynamics*, vol. 54, no. 8, pp. 1031–1052, 2016, doi: 10.1080/00423114.2016.1180404.

[5] E. Katsuyama, M. Yamakado, and M. Abe, "A-state-of-the-art review: toward a novel vehicle dynamics control concept taking the driveline of electric vehicles into account as promising control actuators," *Vehicle System Dynamics*, vol. 59, no. 7, pp. 976–1025, 2021, doi: 10.1080/00423114.2021.1916048.

[6] A. Challa, K. Ramakrushnan, P. V. Gaurkar, S. C. Subramanian, G. Vivekanandan, and S. Sivaram, "A 3-phase combined wheel slip and acceleration threshold algoritm for anti-lock braking in heavy commercial road vehicles," *Vehicle System Dynamics*, doi: 10.1080/00423114.2021.1903048.

[7] L. Castellazzi, A. Tonoli, N. Amati, and E. Galliera, "A study on the role of powertrain system dynamics on vehicle driveability, vol. 55, no. 7, pp. 1012–1028, 2017, doi: 10.1080/00423114.2017.1294699.

[8] M. Comellas, J. Pijuan, M. Nogués, and J. Roca, "Efficiency analysis of a multiple axle vehicle with hydrostatic transmission overcoming obstacles," *Vehicle System Dynamics*, vol. 56, no. 1, pp. 55–77, 2018, doi: 10.1080/00423114.2017.1343954.

[9] Z. Hadas, L. Janak, J. Smilek, "Virtual prototypes of energy harvesting systems for industrial applications," *Mechanical Systems and Signal Processing*, vol. 110, pp. 152–164, 2018, doi: 10.1016/j.ymsssp.2018.03.036.

[10] F. Ji, Y. Pan, Y. Zhou, F. Du, Q. Zhang, and G. Li, "Energy recovery based on pedal situation for regenerative braking system of electric vehicle," *Vehicle System Dynamics*, vol. 58, no. 1, pp. 144–173, 2020, doi: 10.1080/00423114.2019.1567927.

[11] C. Pan, L. Chen, L. Chen, H. Jiang, Z. Li, S. Wang, "Research on motor rotational speed measurement in regenerative braking system of electric vehicle," *Mechanical Systems and Signal Processing*, vol. 66, pp. 829–839, 2016, doi: 10.1016/j.ymssp.2015.06.001.

[12] L. Li, X. Li, X. Wang, Y. Liu, J. Song, and X. Ran, "Transient switching control strategy from regenerative braking to anti-lock braking with a semi-brake-by-wire system," *Vehicle System Dynamics*, vol. 54, no. 2, pp. 231–257, 2016, doi: 10.1080/00423114.2015.1129059.

[13] Y. Shi, B. Li, J. Luo, and F. Yu, "A practical identifier design of road variations for anti-lock brake system," *Vehicle System Dynamics*, vol. 57, no. 3, pp. 336–368, 2019, doi: 10.1080/00423114.2018.1467018.

[14] M. Vignati and E. Sabbioni, "Force-based braking control algorithm for vehicles with electric motors," *Vehicle System Dynamics*, vol. 58, no. 9, pp. 1348–1366, 2020, doi: 10.1080/00423114.2019.1621354.

[15] Z. -G. Zhao, L. -J. Zhou, J. -T. Zhang, Q. Zhu, and J. -K. Hendrick, "Distributd and self-adaptive vehicle speed estimation in the composite braking case for four-wheel drive hybrid electric car," *Vehicle System Dynamics*, vol. 55, no. 5, pp. 750–773, 2017, doi: 10.1080/00423114.2017.1279739.

[16] X. Kong, C. Chen, B. Wen, "Composite synchronization of three eccentric rotors driven by induction motors in a vibrating system," *Mechanical Systems and Signal Processing*, vol. 102, pp. 158–179, 2018, doi: 10.1016/j.ymssp.2017.09.025.

[17] Z. Liu, H. Xiao, P. Khatri, S. Ding, X. Wang, “A study of flux switching linear generator with a novel speed amplified mechanism and its optimization for the maximum power output and minimum cogging force of wave energy conversion,” *Mechanical Systems and Signal Processing*, vol. 166, pp. 108413, 2022, doi: 10.1016/j.ymssp.2021.108413.

[18] T. Sedlacek, D. Odenthal, and D. Wollherr, “Minimum-time optimal control for battery electric vehicles with four wheel-independent drives considering electrical overloading,” *Vehicle System Dynamics*, doi: 10.1080/00423114.2017.1823004.

[19] X. Hu, C. M. Martinez, Y. Yang, “Charging, power management, and battery degradation mitigation in plug-in hybrid electric vehicles: A unified cost-optimal approach,” *Mechanical Systems and Signal Processing*, vol. 87, pp. 4–16, 2017, doi: 10.1016/j.ymssp.2016.03.004.

[20] M. S. Basrah, E. Siampis, E. Velenis, D. Cao, and S. Longo, “Wheel slip control with torque blending using linear and nonlinear model predictive control,” *Vehicle System Dynamics*, vol. 55, no. 11, pp. 1665–1685, 2017, doi: 10.1080/00423114.2017.1318212.

[21] V. K. T. Mantripragada and R. K. Kumar, “Sensitivity analysis of tyre characteristic parameters on ABS performance,” *Vehicle System Dynamics*, vol. 60, no. 1, pp. 47–72, 2022, doi: 10.1080/00423114.2020.1802491.

[22] E. Dinçmen and T. Altınel, "An emergency braking controller based on extremum seeking with experimental implementation," *Int. J. Dynam. Control*, vol. 6, pp. 270–283, 2018, doi: 10.1007/s40435-016-0286-2.

[23] V. Vodovozov, Z. Raud, and E. Petlenkov, "Review on braking energy management in electric vehicles," *Energies*, vol. 14, pp. 4477, 2021, doi: 10.3390/en14154477.

[24] V. Vodovozov, A. Aksjonov, E. Petlenkov, and Z. Raud, "Neural network-based model reference control of braking electric vehicles," *Energies*, vol. 14, pp. 2373, 2021, doi: 10.3390/en14092373.

[25] B. Danquah, S. Riedmaier, Y. Meral, and M. Lienkamp, "Statistical validation framework for automotive vehicle simulations using uncertainty learning," *Appl. Sci.*, vol. 11, pp. 1983, 2021, doi: 10.3390/app11051983.

[26] P. G. Anselma and G. Belingardi, “Multi-objective optimal computer-aided engineering of hydraulic brake systems for electrified road vehicles,” *Vehicle System Dynamics*, doi: 10.1080/00423114.2020.1820048.

[27] L. Pugi, M. Pagliai, A. Nocentini, G. Lutzemberger, A. Pretto, “Design of a hydraulic servo-actuation fed by a regenerative braking system,” *Applied Energy*, vol. 187, pp. 96–115, 2017, doi: 10.1016/j.apenergy.2016.11.047.

[28] P. Walker, B. Zhu, N. Zhang, “Powertrain dynamics and control of a two speed dual clutch transmission for electric vehicles,” *Mechanical Systems and Signal Processing*, vol. 85, pp. 1–15, 2017, doi: 10.1016/j.ymssp.2016.07.043.

[29] Z. Zhao, J. Chen, X. Li, D. Lei, “Downshift decision and process optimal control of dual clutch transmission for hybrid electric vehicles under rapid braking condition,” *Mechanical Systems and Signal Processing*, vol. 116, pp. 943–962, 2019, doi: 10.1016/j.ymssp.2018.07.012.

[30] J. Schoeftner and W. Ebner, “Simulation model of an electrohydraulic-actuated double clutch transmission vehicle: modelling and system design,” *Vehicle System Dynamics*, vol. 55, no. 12, pp. 1865–1883, 2017, doi: 10.1080/00423114.2017.1337207.

[31] J. Torinsson, M. Jonasson, D. Yang, and B. Jacobson, “Energy reduction by power loss minimisation through wheel torque allocation in electric vehicles: a simulation-based approach,” *Vehicle System Dynamics*, doi: 10.1080/00423114.2020.1858121.

[32] J. Jerrelind, P. Allen, P. Gruber, M. Berg, and L. Drugge, “Contributions of vehicle dynamics to the energy efficient operation of road and rail vehicles,” *Vehicle System Dynamics*, vol. 59, no. 7, pp. 1114–1147, 2021, doi: 10.1080/00423114.2021.1913194.

[33] S. Zhou, P. Walker, Y. Tian, and N. Zhang, “Mode switching analysis and control for a parallel hydraulic hybrid vehicle,” *Vehicle System Dynamics*, vol. 59, no. 6, pp. 928–948, 2021, doi: 10.1080/00423114.2020.1737147.

[34] M. Tian, Q. Hu, B. Gao, H. Ding, and H. Chen, “Design and handling dynamic analysis of electric vehicle chassis with yaw direction oscillatable battery pack,” *Vehicle System Dynamics*, doi: 10.1080/00423114.2020.1841902.

Optimizing regenerative braking

ORIGINALITY REPORT

7%	3%	6%	1%
SIMILARITY INDEX	INTERNET SOURCES	PUBLICATIONS	STUDENT PAPERS

PRIMARY SOURCES

1	Erkin Dinçmen, Tunç Altınel. "An emergency braking controller based on extremum seeking with experimental implementation", International Journal of Dynamics and Control, 2016 Publication	1%
2	Submitted to Universitas Muhammadiyah Yogyakarta Student Paper	1%
3	Erkin Dincmen. "Extremum seeking dead-zone pre-compensator for an industrial control system", at - Automatisierungstechnik, 2018 Publication	<1%
4	Kazuki OGAWA, Tatsuhito AIHARA. "Development of two-speed dual-clutch transmission for seamless gear shifting in EVs", Transportation Engineering, 2021 Publication	<1%
5	Kesavan Valis Subramaniyam, Shankar C. Subramanian. "Electrified Vehicle Wheel Slip Control Using Responsiveness of	<1%

Regenerative Braking", IEEE Transactions on Vehicular Technology, 2021
Publication

6	Weida Wang, Xinghua Guo, Chao Yang, Yuanbo Zhang, Yulong Zhao, Denggao Huang, Changle Xiang. "A multi-objective optimization energy management strategy for power split HEV based on velocity prediction", Energy, 2022 Publication	<1 %
7	www.slideshare.net Internet Source	<1 %
8	Fenzhu Ji, Yong Pan, Yu Zhou, Farong Du, Qi Zhang, Guo Li. "Energy recovery based on pedal situation for regenerative braking system of electric vehicle", Vehicle System Dynamics, 2019 Publication	<1 %
9	Jayu Kim, Baeksoon Kwon, Youngnam Park, HyunJong Cho, Kyongsu Yi. "A control strategy for efficient slip ratio regulation of a pneumatic brake system for commercial vehicles", Proceedings of the Institution of Mechanical Engineers, Part D: Journal of Automobile Engineering, 2021 Publication	<1 %
10	ir.library.dc-uoit.ca Internet Source	<1 %

11	Akhil Challa, Karthik Ramakrushnan, Shankar C. Subramanian, Gunasekaran Vivekanandan, Sriram Sivaram. "Analysis Of Thresholds In Rule-Based Antilock Braking Control Algorithms", IFAC-PapersOnLine, 2020 Publication	<1 %
12	Junjiang Zhang, Yang Yang, Datong Qin, Chunyun Fu, Zhipeng Cong. "Regenerative Braking Control Method Based on Predictive Optimization for Four-Wheel Drive Pure Electric Vehicle", IEEE Access, 2021 Publication	<1 %
13	Zhiguo Zhao, Jiayi Chen, Xueyan Li, Dan Lei. "Downshift decision and process optimal control of dual clutch transmission for hybrid electric vehicles under rapid braking condition", Mechanical Systems and Signal Processing, 2019 Publication	<1 %
14	www.mdpi.com Internet Source	<1 %
15	J. Schoeftner, W. Ebner. "Simulation model of an electrohydraulic-actuated double-clutch transmission vehicle: modelling and system design", Vehicle System Dynamics, 2017 Publication	<1 %

16	Xiangxi Kong, Changzheng Chen, Bangchun Wen. "Composite synchronization of three eccentric rotors driven by induction motors in a vibrating system", Mechanical Systems and Signal Processing, 2018 Publication	<1 %
17	Yue Shi, Bin Li, Jiannan Luo, Fan Yu. "A practical identifier design of road variations for anti-lock brake system", Vehicle System Dynamics, 2018 Publication	<1 %
18	ro.uow.edu.au Internet Source	<1 %
19	web-tools.uts.edu.au Internet Source	<1 %

Exclude quotes	Off	Exclude matches	Off
Exclude bibliography	On		